Nuclear Engineering and Technology 54 (2022) 2748–2754

Contents lists available at ScienceDirect

Nuclear Engineering and Technology

journal homepage: www.elsevier.com/locate/net

Technical Note

Feasibility study of β-ray detection system for small leakage from reactor coolant system

Jaeyeong Jang [a], Jae Young Jeong [c], Junesic Park [b], Young-Sik Cho [b], Kihong Pak [c], Yong Kyun Kim [c, *]

[a] Korea Institute of Nuclear Nonproliferation and Control, Daejeon, South Korea
[b] Korea Atomic Energy Research Institute, Daejeon, South Korea
[c] Department of Nuclear Engineering, Hanyang University, Seoul, South Korea

ARTICLE INFO

Article history:
Received 29 September 2020
Received in revised form
29 November 2021
Accepted 24 January 2022
Available online 29 January 2022

Keywords:
Beta-ray detector
Leakage detection system
^{16}N
Reactor coolant system
Unidentified leakage
RCS leakage

ABSTRACT

Because existing reactant coolant system (RCS) leakage detection mechanisms are insensitive to small leaks, a real-time, direct detection system with a detection threshold below 0.5 gpm·hr^{-1} was studied. A beta-ray detection system using a silicon detector with good energy resolution for beta rays and a low gamma-ray response was proposed. The detection performance in the leakage condition was evaluated through experiments and simulations. The concentration of ^{16}N in the coolant corresponding to a coolant leakage of 0.5 gpm was calculated using the analytic method and ORIGEN-ARP. Based on the concentration of ^{16}N and the measurement of the silicon detector with ^{90}Sr/^{90}Y, the beta-ray count rate was estimated using MCNPX. To evaluate the effect of gamma rays inside the containment building, the signal-to-noise ratio (SNR) was calculated. To evaluate the count rate ratio, the radiation field inside the containment building was simulated using MCNPX, and response evaluation experiments were performed using beta and gamma rays on the silicon detector. The expected beta-ray count rate at 0.5 gpm leakage was 7.26 × 10^5 counts/sec, and the signal-to-background count rate ratio exceeded 88 for a transport time of 10 s, demonstrating its suitability for operation inside a reactor containment building.

1. Introduction

Currently, leakage detection methods used for reactor coolant systems (RCS) in nuclear power plants are based on the measurement of humidity, temperature, and radioactivity inside the reactor containment building, along with sump tank level. These systems enable the detection of coolant leakage of up to 1 gpm (gallons per minute) in 1 h [1,2]. However, for small leakages, existing systems are vulnerable to leakage detection owing to the imperceptible variation in parameters such as temperature, humidity, radioactivity, and level in the sump tank, along with error sources such as phase changes and intermediate condensation of vapor in the containment. In 2017, due to such vulnerabilities, 306 L of coolant leaked from Kori Unit 4 because leakage detection was delayed for more than 12 h [3]. A portion of nuclear accidents result from small leakages. To increase nuclear power plant safety, a system with a lower detection threshold (e.g., 0.5 gpm) is required. Considering this, a detection system with ^{16}N in the coolant set as the target nuclide was studied. ^{16}N gamma-ray monitors were introduced to the nuclear reactor to monitor primary to secondary leakage in the steam generator [4]. However, if ^{16}N gamma-ray monitors are installed inside the containment building for leak detection, a high background signal will be generated by the high-energy and high-intensity gamma-ray field inside the containment building. Therefore, it was considered that the application of ^{16}N gamma monitor would be difficult for detecting small leakage of RCS, and a beta-ray detection system with a silicon detector placed inside the containment building was suggested [5].

In this study, the count rate of the beta-ray detection system for a coolant leakage of 0.5 gpm was calculated through both experiments and simulations because ^{16}N could not be used for experiments in a laboratory environment due to the short half-life and high-energy gamma-ray emission. First, the simulation reliability was evaluated by comparing the energy spectra of the simulation and the experiment with the ^{90}Sr/^{90}Y source under simple geometric conditions. Next, the experiment for the gamma-ray response rate evaluation of the silicon detector was performed

* Corresponding author.
E-mail address: ykkim4@hanyang.ac.kr (Y.K. Kim).

https://doi.org/10.1016/j.net.2022.01.028

under the same conditions. Then, the count rate of ^{16}N beta-ray in the detection chamber was calculated using the MCNP simulation code. Based on the simulations, the feasibility of a beta-ray detection system using a silicon detector for small leakage was discussed by comparing the signal count rate from the leaked coolant to the background gamma-ray count rate.

2. Materials and methods

2.1. Reliability evaluation of MCNPX simulation by comparison with experimental beta-ray spectrum

In previous literature, ^{16}N was selected as the target nuclide to determine the RCS leakage because ^{16}N was 93% of the total radioactive concentration inside the RCS and emitted both high-energy gamma rays and beta-rays, with 6.1-MeV and 7.1-MeV gamma-rays and 10.42 MeV beta-rays [5].

As shown in Fig. 1, the beta-rays emitted from ^{16}N have an endpoint energy of 10.42 MeV, and the detection performance of the silicon detector for beta rays in the high-energy range must be verified. However, ^{16}N has a short half-life of 7.13 s and emits high-energy gamma rays, rendering it unsuitable for experiments in a laboratory environment. Therefore, the evaluation experiment of the performance of the silicon detector using ^{16}N was replaced with MCNPX simulation. Before the simulation with ^{16}N, the reliability of the MCNPX simulation of the spectrum measurement of the silicon detector for the beta-rays was evaluated.

Because the source that emits the highest energy beta-rays among the beta-ray check sources is ^{90}Sr/^{90}Y, the reliability of the MCNPX simulation was verified by comparing the measured value with a ^{90}Sr/^{90}Y source and the simulation under the same conditions. The endpoint energy of beta rays emitted from ^{90}Sr/^{90}Y is 2.28 MeV, as shown in Fig. 2.

The silicon detector used in the experiment with a ^{90}Sr/^{90}Y source is an ORTEC ULTRA ion-implanted detector, and the area and minimum thickness of the silicon depletion layer are 1200 mm^2 and 300 μm, respectively [6]. A schematic and photograph of the experimental setup are shown in Figs. 3 and 4, respectively, and the experimental conditions are shown in Table 1. The disk source of ^{90}Sr/^{90}Y was located 3 cm from the surface of the silicon detector. A silicon detector was connected to an ORTEC 142A preamplifier and 572A amplifier and 928 multichannel buffer with 1024 channels. The beta-ray energy spectra were measured for 1 h. Energy calibration for the multichannel buffer was performed with ^{210}Po, which emits alpha particles of energy 5.30 MeV. The alpha particle

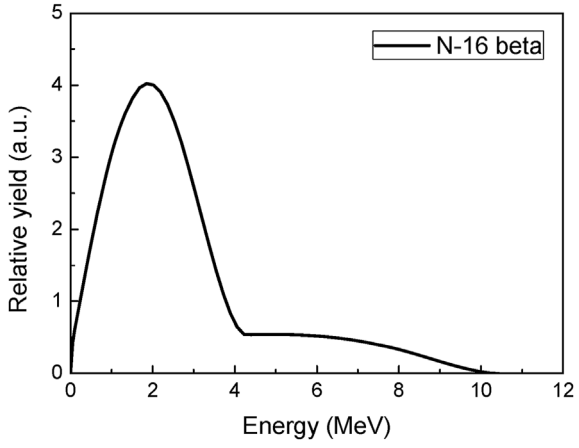

Fig. 1. Beta-ray spectrum of ^{16}N.

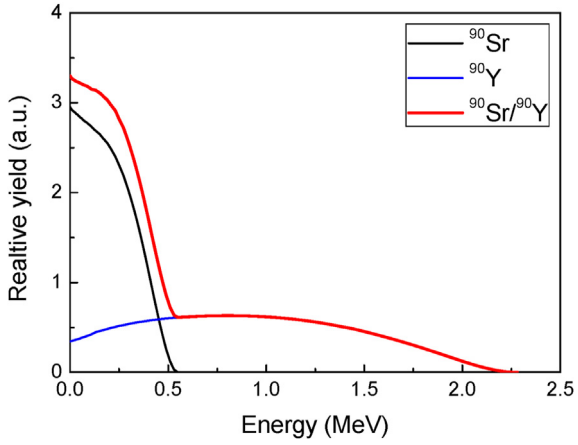

Fig. 2. Beta-ray spectra of ^{90}Sr and the daughter nucleus ^{90}Y.

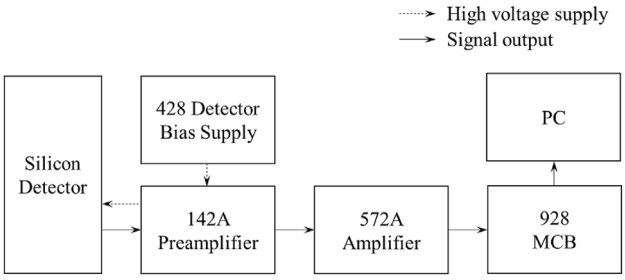

Fig. 3. Schematic of experiment using a check source.

peak appeared at the 584th channel while channel 0 was treated as a 0-MeV peak. Through this pre-measurement, the multichannel buffer was calibrated to 0.009082 MeV/channel. The MCNPX simulation was performed using the geometric model described in Fig. 5. The structure of the silicon detector simulated that of the ORTEC ULTRA Ion-Implanted Detector. The distance between the detector and the ^{90}Sr/^{90}Y source was 3 cm, similar to the experiment. Considering the attenuation of beta-rays in air, the surrounding space was set with an air density of 0.001205 g/cm^3. The beta-ray energy spectra were obtained using an F8 tally (pulse height tally) card. The tally was set for the depletion layer cell of the silicon detector where electrons were incident. Gaussian energy broadening (GEB) was not considered because the silicon detector has good energy resolution for charged particles. According to the certificate of conformance quality assurance data sheet of the silicon detector, the energy resolution was approximately lower than 0.67% with the ^{241}Am alpha-ray source, which is negligible. The energy resolution for a beta-ray in the silicon detector is also expected to be negligible because all experimental values obtained using light ions and fast electrons seem to be fairly close to the detector calibrations carried out using alpha particles [7–9].

2.2. Response evaluation of silicon detector for beta and gamma-ray

Considering the contribution of the gamma-ray background to the silicon detector, an experiment was performed using beta and gamma sources. The experimental setup was the same as that of the previous experiment described in section 2.1. ^{90}Sr/^{90}Y and gamma sources such as ^{22}Na, ^{60}Co, and ^{137}Cs were used, and the experiment was performed under the conditions shown in Table 2. The response of the silicon detector was calculated in the total energy

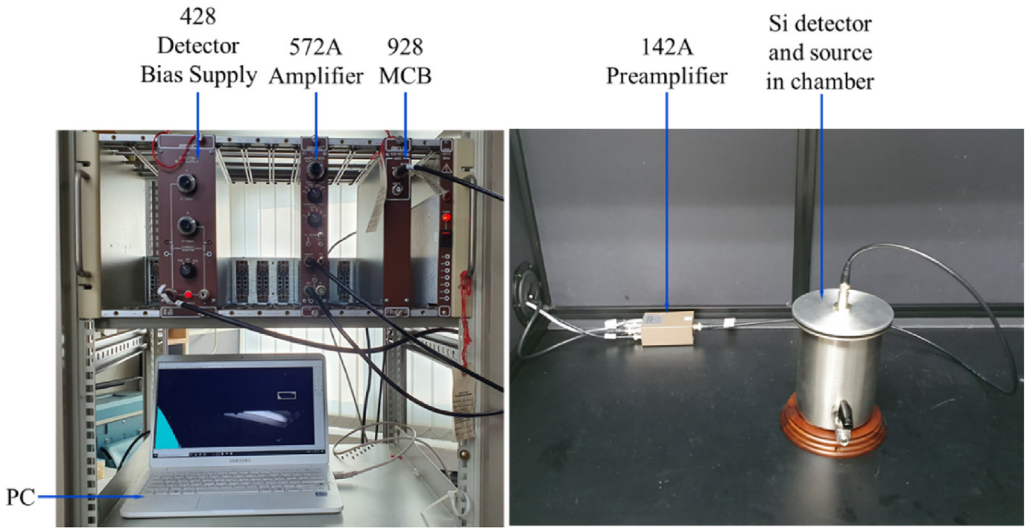

Fig. 4. Picture of the experimental setup.

Table 1
Experimental conditions for $^{90}Sr/^{90}Y$ beta-ray measurement.

Temperature	25 °C
Pressure	1 atm
Source	$^{90}Sr/^{90}Y$ ($E_{Endpoint}$: 2.3 MeV, 0.1 μCi)
Distance between source and silicon detector	3 cm
Bias voltage on detector	+110 V
Shaping time of amplifier	1 μsec
Gain of amplifier	50
Conversion gain (MCB channel No.)	1024
Measurement time	3600 s

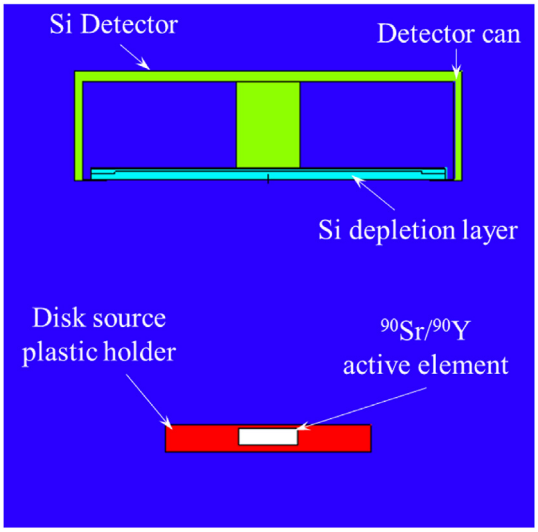

Fig. 5. Vertical cross-section of the MCNPX geometry model of silicon detector and $^{90}Sr/^{90}Y$ check source.

range using Eq. (1). The probability of entering the detector is the ratio of the radiation incident on the detector to the radiation traveling isotropically. Therefore, the probability was calculated as the ratio of the solid angle incident on the detector to the total solid angle of 4π.

Table 2
Experimental condition of measurement with beta and gamma sources.

Temperature	25 °C
Pressure	1 atm
Source	β-source: $^{90}Sr/^{90}Y$ ($E_{Endpoint}$: 2.28 MeV, 0.1 μCi) γ-source: ^{22}Na (1.27 MeV, 5.65 μCi) ^{137}Cs (0.662 MeV, 10.53 μCi) ^{60}Co (1.17/1.33 MeV, 0.91 μCi)
Distance between source and detector	3 cm
Bias voltage on detector	+110 V
Shaping time of amplifier	1 μsec
Gain of amplifier	50
Conversion gain (MCB channel No.)	1024
Measurement time	3600 s

$$Response = \frac{Total\ Count}{Incident\ rate\ of\ radiation \times Measurement\ time} \quad (1)$$

$$Incident\ rate\ of\ radiation = Emission\ rate\ of\ radiation \times Probability\ of\ entering\ the\ detector$$

2.3. Estimation of ^{16}N beta-ray count rate of silicon detector at the detection chamber in a nuclear power plant

The ^{16}N beta-ray spectrum on the silicon detector was simulated using MCNPX, and the count rate was estimated using the response of the silicon detector. The response of the silicon detector to radiation was defined as the occurrence count rate per number of incident radiation. The response was derived from the $^{90}Sr/^{90}Y$ measurement experiment and calculated using Equation (1).

The beta rays emitted from ^{16}N have an endpoint energy of 10.42 MeV and an average energy of 2 MeV, which is approximately 20% of the endpoint energy. However, most of the other nuclides present inside the reactor coolant emit beta-rays with an average energy lower than 2 MeV [4,5]. To facilitate the differentiation from other nuclides in the reactor coolant, the region of interest was assigned as more than 2 MeV. In the measurement experiment of $^{90}Sr/^{90}Y$, the same ratio of the energy region was applied to calculate the count rate and count rate conversion factor from 0.46 MeV.

Next, the concentration of ^{16}N in the leakage coolant was calculated based on Equation (2) and the data of nuclide activity inside the coolant during normal operation of the final safety analysis report (FSAR) of APR1400 [4,10]. The value of V (computational domain volume) was determined to be 2955 cm^3 based on the assumption that the distance between the RCS pipe of APR1400 and the insulation was 1 mm, and the distance between the suction holes in the sampling pipe was 1 m [4]. It was assumed that the concentration of radioactivity in the computational domain was uniform, and the leaked ^{16}N was assumed to be gaseous as the pressure was lower than inside the RCS pipe. It was also assumed that the leakage coolant in the computational domain passed over 100% of the sampling pipe owing to the suction of the sampling pipe. The value of the leakage rate (L) was assumed to be 0.5 gpm, which is the target value of the leakage detection system. The values of the plate-out factor (P_f) and atmosphere removal rate (Q) were assumed to be 0. This is because ^{16}N is a non-precipitating material, and the computational domain is a nearly closed space.

$$V\frac{dA}{dt} = LC - \lambda AC - P_f LC - QA \tag{2}$$

V = Computational domain volume (cm^3)A = Concentration of radioisotope in the computational domain

$$radioisotope in the computational domain \left(\mathrm{Bq} \,/\, cm^3\right)$$

C = Concentration of radioisotope in the reactor coolant

$$coolant \left(\mathrm{Bq} \,/\, cm^3\right)$$

L = Leakage rate of reactor coolant $(cm^3/\mathrm{min})\lambda$ = Decay constant of isotope $(\mathrm{min}^{-1})P_f$ = Plateout factor, fration of leaking radioisotope that is remoned by plateout

$$of leaking radioisotope that is remoned by plateout$$

Q = Atmosphere removal rate of computational domain

$$domain \left(cm^3 \,/\, \mathrm{min}\right)$$

The simplified structure of the RCS leakage detection system is illustrated in Fig. 6. Using an air pump, the leaked coolant with ^{16}N reaches the detection chamber quickly. The variation of concentration over the transport time was calculated using the calculated concentration and the ORIGEN-ARP (Automatic Rapid Processing) code. The ORIGEN-ARP code uses the pre-installed decay data to calculate the changes in the radioisotope concentration and gamma-ray spectrum at the time specified by the user. The number of beta-rays entering the silicon detector when the leaked coolant arrived at the detection chamber was calculated using MCNPX and the results of the ORIGEN-ARP code [11,12]. Fig. 7 shows the geometry of the MCNPX model. The number of beta-rays entering the silicon detector was estimated as the value of the tracks entering from the MCNPX simulation output. At this time, the activity of ^{16}N inside the detection chamber differed depending on the concentration of ^{16}N according to the transport time using FM tally. The volume of the detection chamber which was surrounded by lead shielding was 1710 cm^3, as shown in Fig. 7. The count rate of the silicon detector was estimated based on the number of beta-rays entering the silicon detector. The count rate was calculated using Equation (3).

$$\begin{aligned} Total\ Count\ rate &= \frac{Total\ Count}{Measurement\ time} \\ &= Response \times Incident\ rate\ of\ radiation \end{aligned} \tag{3}$$

2.4. Estimation of signal to background ratio using MCNPX simulation

To evaluate the background gamma radiation in the annular space, which is expected to be the installation location of the silicon

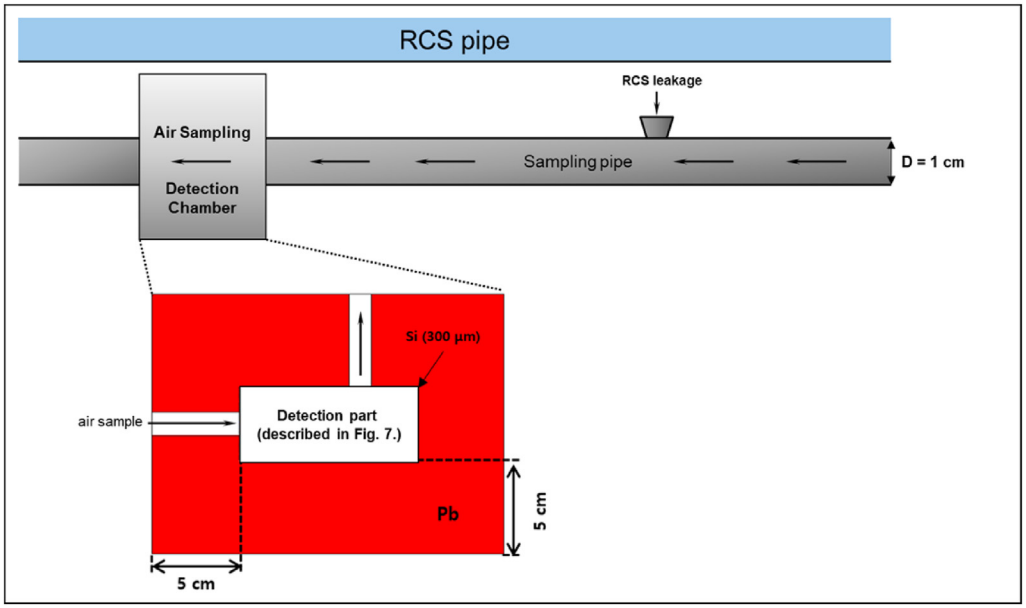

Fig. 6. Simplified structure of the RCS leakage detection system for small leakage using beta-ray detector.

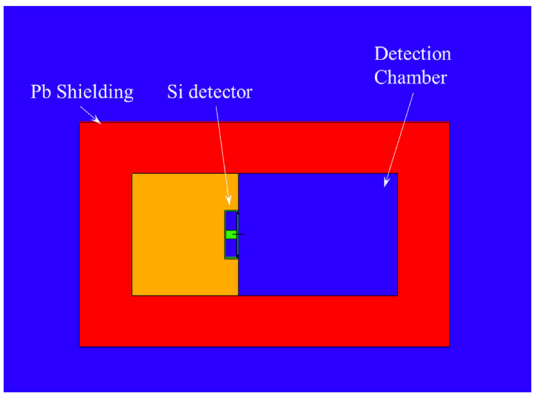

Fig. 7. Cross-section of the MCNPX geometry model of Si detector and configuration.

detector, the radiation field was simulated using MCNPX. The annular space was included in zone 6, where the design criteria dose rate was set to 10 mSv/h [4]. The design criterion consists of the dose due to neutrons, gamma rays from the nuclear reactor, and secondary gamma rays induced by neutrons reacting with the internal structures. It was assumed that the background in the detector was contributed solely by gamma rays because their effect on signals for the silicon detector is relatively greater than that of neutrons. To model the background gamma rays in the annular space, the source was designated based on the neutron flux and gamma-ray flux data near the reactor vessel [4]. Then, as shown in Fig. 8, structures such as the concrete wall of the reactor were reconstructed, and the energy distribution of the gamma-ray flux produced by the reaction with the structural material was calculated using F4 tally. The gamma-ray flux distribution in the annular space was derived by summing up the primary gamma-rays from the reactor and the secondary gamma-rays. The number of gamma rays entering the silicon detector was calculated when the intensity of the source was adjusted such that the dose rate due to the gamma ray of the calculated energy distribution was 10 mSv/h.

The expected signal-to-background ratio was derived by applying the experimental response to the number of beta rays and gamma rays entering the silicon detector using MCNPX simulation.

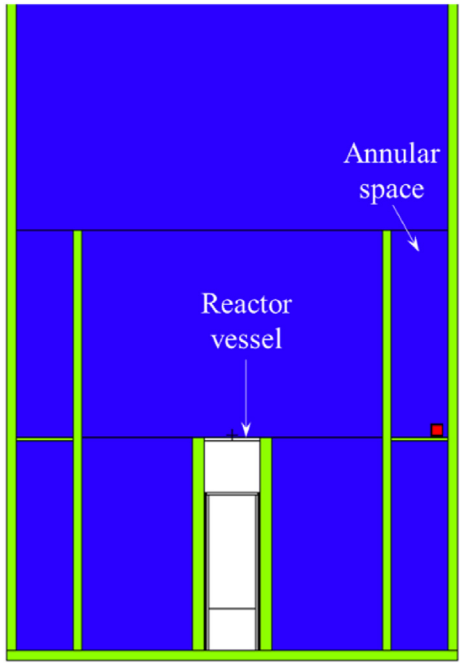

Fig. 8. MCNPX geometry model of structures inside the containment building.

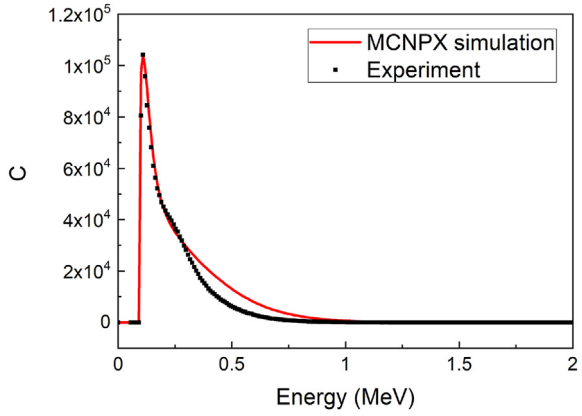

Fig. 9. Energy spectra of $^{90}Sr/^{90}Y$ obtained through experiment and MCNPX simulation.

3. Result and discussion

Fig. 9 shows the energy spectra obtained from the experiment and the MCNPX simulation with the $^{90}Sr/^{90}Y$ source under the conditions described in Section 2.1. The energy spectrum of the MCNPX simulation was normalized based on the experimental energy spectrum, assuming that the total counts of the simulation and the experiment were the same. As shown in Fig. 9, the count of the simulation spectrum is higher than that of the experimental spectrum in the range of 0.30 MeV–1 MeV. However, it seems to be a good agreement based on the shape of the spectrum and the peak channel. Fig. 9 shows the different energy spectrum trends shown in Fig. 2. This is due to the thickness of the depletion layer of the silicon detector. The CSDA range of a 2 MeV electron is 5.099 mm such that only the partial energy of the electrons is deposited on the detector [13].

In the $^{90}Sr/^{90}Y$ measurement experiment, the total counts were obtained at the value of $1.24 \times 10^5 \pm 353$ counts in the range of 0.46 MeV–2.28 MeV. The activity of the $^{90}Sr/^{90}Y$ source was 0.098 μCi, and $^{90}Sr/^{90}Y$ generated two beta-rays per decay. As the solid angle of incidence on the detector is 0.93 steradian geometrically, the probability of entering the detector was calculated to be approximately 0.07. Therefore, the response was calculated to be 6.79×10^{-2} counts/β, which is almost the same as the probability.

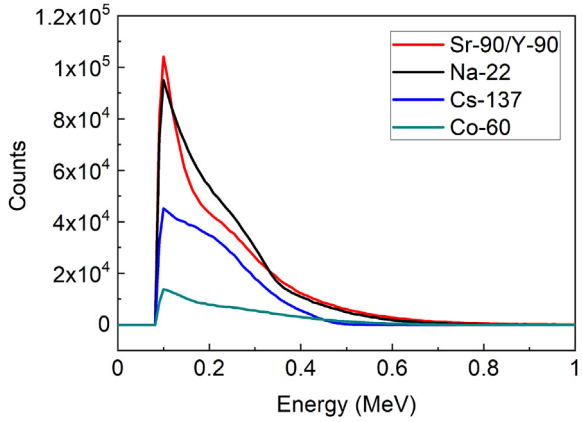

Fig. 10. Energy spectra of silicon detector for beta- and gamma-ray sources.

Table 3
Total count and response of Si detector to beta-ray and gamma-ray.

Source	Type	Total count	Activity [μCi]	Incident rate of radiation [#/sec]	Efficiency of Si detector [Count/#]
$^{90}Sr/^{90}Y$	pure β	1618353 ± 1272	0.098	507.64	8.86×10^{-1}
^{22}Na	pure γ	1704428 ± 1306	5.65	14633.50	3.24×10^{-2}
^{137}Cs	pure γ	939295 ± 969	10.53	27272.70	9.57×10^{-3}
^{60}Co	pure γ	287919 ± 537	0.90	4662	1.72×10^{-2}

Table 4
Summary of signal to background count rate ratio calculation results.

Type of signal	Type of radiation	Entering number of radiation [#/sec]	Response of Si detector [Count/#]	Count rate [count/sec]	Ratio
Leakage signal	^{16}N beta-ray	1.07×10^{6}	8.86×10^{-1}	9.48×10^{5}	100
Background signal	Background gamma-ray	3.32×10^{5}	3.24×10^{-2}	1.07×10^{4}	1.13

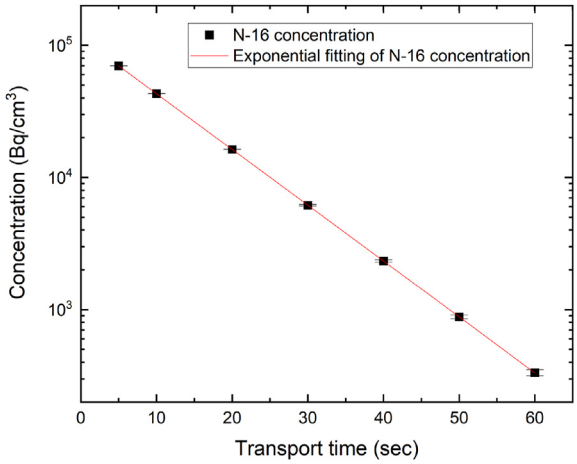

Fig. 11. Concentration of ^{16}N in leaked coolant as a function of transport time.

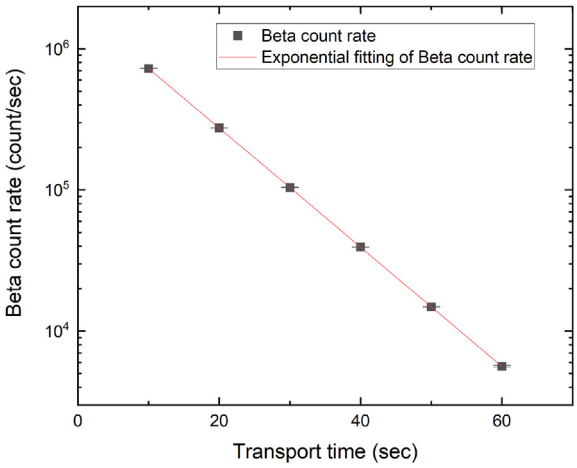

Fig. 12. Count rate of beta-ray detection system as a function of transport time.

The measured spectra of the silicon detector for the $^{90}Sr/^{90}Y$, ^{22}Na, ^{137}Cs, and ^{60}Co sources are shown in Fig. 10. The response of the silicon detector for $^{90}Sr/^{90}Y$, ^{22}Na, ^{137}Cs, and ^{60}Co sources was respectively 8.86×10^{-1}, 3.24×10^{-2}, 9.57×10^{-3}, and 1.72×10^{-2} and summarized in Table 3. For a conservative estimate, the efficiency of the silicon detector derived from ^{22}Na, the largest value among the gamma-ray efficiency, was considered hereafter as the gamma-ray response (see Table 4).

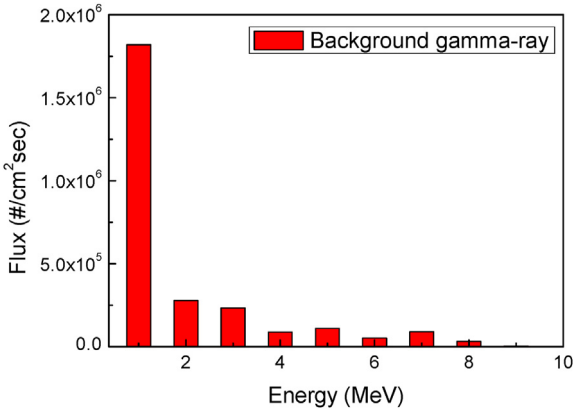

Fig. 13. Energy distribution of gamma flux in Annulus zone (using MCNPX code).

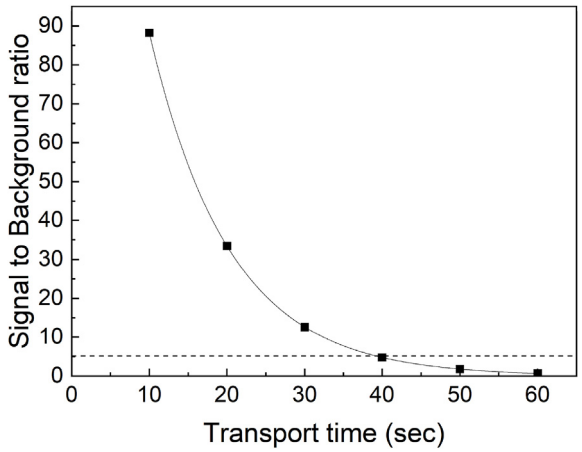

Fig. 14. Signal to background count rate ratio of beta-ray detection system using silicon detector.

Fig. 11 shows the activity of ^{16}N in the leaked coolant calculated using Equation (2) and the ORIGEN-ARP code. As the transport time increased, the activity of ^{16}N decreased rapidly. The number of beta-rays of ^{16}N from the chamber volume was 1.07×10^{7} β/sec using MCNPX simulation at 10 s of transport time. Fig. 12 shows the beta-ray count rate of the silicon detector as the transport time increased. The beta-ray count rate was 7.26×10^{5} counts/s by applying 6.79×10^{-2} counts/β of response of the silicon detector at 10 s of transport time. When the transport time was 60 s, the count rate was 5.62×10^{3} counts/s, which was approximately 12 times

greater than the count rate of 4.50×10^2 counts/s in the $^{90}Sr/^{90}Y$ measurement experiment.

Fig. 13 shows the energy distribution of the background gamma-ray flux in the annular space. The number of background gamma rays entering the silicon detector was calculated at 3.32×10^5 γ/sec. The number of beta-rays entering the silicon detector from ^{16}N in the leaked coolant was calculated as 1.07×10^6 β/sec.

As a result of the silicon detector response obtained from the experiment, the ratio of the signal count rate due to the ^{16}N of the leaked coolant and the background count rate due to the background gamma rays was calculated as 100 : 1.13. When the energy range of interest was assigned to be more than 2 MeV as mentioned in Section 2.3, the ratio was calculated as 100:0.48, and the difference became larger owing to the background gamma energy distribution.

Fig. 14 presents the signal to background count rate ratio of beta-ray detection system using silicon detector as the transport time increases. At 10 s of the transport time, the signal to background count rate ratio of the beta-ray detection system was 88.23. Although the standard deviation could not be considered, it is a value higher than 5, which was sufficient to detect leakage of RCS in the existing system [14]. The signal to background count rate ratio of silicon detector reached approximately 4.78 at 40 s of transport time and was comparable to the ratio in the existing RCS leakage detection system [14].

4. Conclusion

Existing RCS leak detection systems have a weakness in detecting small amounts of leakage. In this study, a beta-ray detection system that uses a silicon detector to mitigate this was proposed. The feasibility of this silicon detector inside the reactor containment building was evaluated indirectly through the MCNP simulation and experiment for detecting small leakage of the primary system coolant.

The beta-ray count rate was estimated as 7.26×10^5 counts/s at 10 s of transport time and 5.62×10^3 counts/s at 60 s of transport time. They were obtained through experiments and the activity of target nuclide ^{16}N calculated using ORIGEN-ARP and MCNPX codes. The signal count from ^{16}N in the leaked coolant is 88.23 times higher than the background count rate at 10 s of transport time. The count rate of the signal is 4.78 times higher than the background count rate at 40 s of transport time, a clear indication of the capability to detect an RCS leakage of 0.5 gpm.

Existing RCS leakage detection systems have a detection limit of 1 gpm in 1 h. Moreover, existing systems have a longer response time for airborne gaseous radioactivity because of the improvement in fuel integrity [15]. On the other hand, in the new beta-ray detection system, ^{16}N, which is an activation product independent of fuel integrity, was selected as the target nuclide, and the response time was reasonably short because of the fast sampling pipe system that uses an air pump. Additionally, the capability to detect the RCS leakage of less than 0.5 gpm is verified as the signal count rate from the leaked coolant is significantly higher than the background count rate. Therefore, a beta detection system that uses a silicon detector can be considered an appropriate choice suitable for detecting small leakage of coolant inside the reactor containment building.

Declaration of competing interest

The authors declare that they have no known competing financial interests or personal relationships that could have appeared to influence the work reported in this paper.

Acknowledgment

This work was supported by the Korea Institute of Energy Technology Evaluation and Planning (KETEP) grant funded by the Korean government (MOTIE) (20181510102340, Development of a real-time detection system for unidentified RCS leakage less than 0.5 gpm).

References

[1] U.S., Nuclear Regulatory Commission, Regulatory Guide 1.45 Guidance on Monitoring and Responding to Reactor Coolant System Leakage, May 2008.
[2] C. King, In Materials Reliability Program: Survey of On-Line PWR Primary Coolant Leak Detection Technologies (MRP-187), EPRI, 2005.
[3] Operational Performance Information System for Nuclear Power Plant, http://opis.kins.re.kr, KINS.
[4] Korea Hydro, Nuclear power Co Ltd, ShinKori Nuclear Unit 3,4 Final Safety Analysis Report, 2015.
[5] J. Jang, T. Schaarschmidt, Y.K. Kim, Feasibility study of beta detector for small leak detection inside the reactor containment, J. Radiat. Prot. Res. 43 (2018) 154–159.
[6] ORTEC Radiation Detectors, https://www.ortec-online.com/products/radiation-detectors.
[7] R.H. Pehl, F.S. Goulding, D.A. Landis, M. Lenzlinger, Accurate determination of the ionization energy in semiconductor detectors, Nucl. Instrum. Methods 59 (1968), 55-45.
[8] C. Canali, M. Martini, G. Ottaviani, A. Alberigi Quaranta, Measurements of the average energy per electron-hole pair generation in silicon between 5-320 K, IEEE Trans. Nucl. Sci. NS- 19 (4) (1972) 9–19.
[9]] R.D. Ryan, Precision measurements of the ionization energy and its temperature variation in high purity silicon radiation detectors, IEEE Trans. Nucl. Sci. NS- 20 (1) (1973) 473–480.
[10] Instrument Society of America, Standard for light water reactor coolant pressure boundary leak detection, ISA-67.3-1982..
[11] I.C. Gauld, et al., ORIGEN-ARP: Automatic Rapid Processing for Spent Fuel Depletion, Decay, and Source Term Analysis, NUREG/CR-0200, 2004. ORNL/NUREG/CSD-2/V1/R7.
[12] D.B. Pelowitz (Ed.), MCNPX User's Manual Version 2.7.0, LA-CP-11-00438, Los Alamos National Laboratory, 2011.
[13] M.J. Berger et al., ESTAR, PSTAR, and ASTAR: Computer Programs for Calculating Stopping-Power and Range Tables for Electrons, Protons, and Helium Ions, http://physics.nist.gov/Star.
[14] Wu-Hung Peng, Particulate activity accumulated on A moving filter and RCS leak detection, Health Phys. 103 (2 Suppl 2) (2012) 174–178.
[15] U.S. Nuclear Regulatory Commission, Information Notice 2005-24: Non-conservatism in Leakage Detection Sensitivity, Washington, DC, August 3, 2005.